ELSEVIER

Catena 47 (2002) 227–243

CATENA

www.elsevier.com/locate/catena

Raindrop-induced and wind-driven soil particle transport

G. Erpul [a,*], L.D. Norton [a], D. Gabriels [b]

[a] *USDA-ARS National Soil Erosion Research Laboratory, 1196 SOIL Bldg., Purdue University, West Lafayette, IN 47907-1196, USA*

[b] *Department of Soil Management and Soil Care, Ghent University, Coupure Links 653, B 9000 Ghent, Belgium*

Received 30 May 2000; received in revised form 5 July 2001; accepted 7 September 2001

Abstract

A wind tunnel study under wind-driven rains was conducted to determine the combined effect of rain and wind on the rainsplash transport process. The rains driven by horizontal wind velocities of 6, 10 and 12 m s^{-1} were applied to three agricultural soils packed into a 20 × 55-cm soil pan placed at both windward and leeward slopes of 4.0°, 8.5° and 11.3°. Transport rates were measured by trapping the splashed particles at set distances in the upslope and downslope directions, respectively, for windward and leeward slopes. Rainsplash transport under wind-driven rains was adequately described ($R^2 = 0.93$) by relating the transport rate to the rain impact pressure and wind shear velocity by log–linear regression technique. Average trajectory of a raindrop-induced and wind-driven particle was also adequately predicted by the momentum loss per unit time per unit length of travel (u_*^2/g). The travel distance is found to be three times greater than the path of a typical saltating sand grain.

Keywords: Wind-driven rain; Rain impact pressure; Wind shear velocity; Rainsplash transport

1. Introduction

Rainsplash transport of soil particles in windless rains has been studied in detail (Van Heerden, 1967; Moeyersons and De Ploey, 1976; Morgan, 1978; Poesen and Savat, 1981; Poesen, 1985, 1986; Wright, 1987). The overall result of these studies is that the contribution of rainsplash transport is very small when compared to overland flow transport. Because of this, rainsplash transport has been most widely neglected in recent

* Corresponding author. Tel.: +1-765-494-6596; fax: +1-765-494-5948.
E-mail address: erpul@purdue.edu (G. Erpul).

0341-8162/02/$ - see front matter
PII: S0341-8162(01)00182-5

erosion models (Kinnell, 1991), and therefore, there is a general tendency that the soil detached by rainsplash will be subsequently transported by overland flow (Hairsine and Rose, 1991; Parsons et al., 1994; Sharma et al., 1995). On the other hand, it is well documented that rainsplash can cause net transportation in the prevailing wind direction when the rain and wind coincide (Jungerius et al., 1981; Moeyersons, 1983; Jungerius and Dekker, 1990; De Lima et al., 1992). However, none of the current erosion model has attempted to model the extent and magnitude of rainsplash transport under wind-driven rain.

Soil detachment under wind-driven rain differs from that under windless rain (Lyles et al., 1969, 1974; Disrud and Krauss, 1971). Since wind-driven raindrop falls with an increased resultant velocity (Umback and Lembke, 1966; Pedersen and Hasholt, 1995; Erpul et al., 2000) and strikes the soil surface with an angle deviated from the vertical (Van Heerden, 1964; De Lima, 1989), its vertical impact pressure differs from that of the vertically falling raindrop. No impact pressure acts on a soil surface by a raindrop with a velocity v regardless of its magnitude that is parallel to the surface, and the soil surface experiences a maximum impact pressure when raindrops fall perpendicular to the soil surface (Ellison, 1947). In general, if a raindrop falls at an angle of incidence i, only the component of velocity $v \cos i$ (m s^{-1}) normal to the soil surface gives rise to an impact pressure (Heymann, 1967; Springer, 1976), therefore:

$$p_d = \rho v^2 \cos^2 i \tag{1}$$

where p_d is the impact pressure of a raindrop (N m^{-2}), and ρ is the raindrop density (kg m^{-3}). The raindrop impact frequency also depends upon the angle of the rainfall incidence (Sharon, 1980; De Lima, 1990):

$$I = R \cos i \tag{2}$$

where I is the rainfall intensity (mm h^{-1}) intercepted by a sloping surface, and R is the rainfall intensity (mm h^{-1}) with respect to a plane normal to the rain vector. Thus, the frequency of the wind-driven raindrops on sloping surfaces differs depending on the wind direction and velocity. If raindrops with Ξ number (#) strike a soil surface, the total rain impact pressure Γ (N m^{-2}) is described by:

$$\Gamma = \Xi p_d \tag{3}$$

If we assume that the effect of the wind shear stress on the detachment is insignificant when compared to the effects of the impacting raindrops, the detachment rate (D) at which soil particles are supplied into the air is a linear function of the raindrop impact pressure:

$$D = K\Gamma \tag{4}$$

where K is the soil detachment factor. The maximum soil detachment rate for the case of the rainsplash transport occurs when there is no water running on the soil surface (Moss and Green, 1983; Moeyersons, 1983). Before the onset of runoff, soil shear strength decreases with increasing soil water content, and at saturation, the soil resistance to the detachment attains a minimum (Al-Durrah and Bradford, 1981; Poesen, 1981; Schultz et

al., 1985; Parsons et al., 1994). After the start of the runoff and ponding, the rainsplash rate falls to a large extent through the flow depth range of 0–2 mm, and beyond it becomes negligible (Ghadiri and Payne, 1981; Moss and Green, 1983; Torri et al., 1987).

Similarly, soil transport under wind-driven rain differs from that under windless rain (Jungerius et al., 1981; Moeyersons, 1983; Jungerius and Dekker, 1990; De Lima et al., 1992). Wind, as well as overland flow, is another possible factor capable of transporting the detached particles. When raindrops are driven at an angle, they do not strike perpendicularly to the surface but tend to splash soil particles in a single direction (Ellison, 1947). De Lima (1989) demonstrated the significance of wind mainly affecting the droplet splash anisotropy, which determines the direction and extent of rainsplash erosion.

Consequently, our approach to the rainsplash transport process under wind-driven rain is based on the concept that once lifted off by the raindrop impact, the soil particles entrained into the splash droplets travel some distance, which varies directly with the shear velocity. The raindrop impacts induce the process that wind would otherwise be incapable of transporting. Therefore, the raindrop-induced and wind-driven transport process can be described by:

$$Q_{\mathrm{wd}} = f(\Gamma, u_*) \tag{5}$$

where Q_{wd} is the raindrop-induced and wind-driven transport, and u_* is the wind shear velocity. By the time that runoff occurs, this process will produce the net transport from bare areas to water-covered surfaces and provides the first stage of the transport sequence of soil erosion from interrill areas. Our study thus hypothesizes that in wind-driven rains, the interrill transport process can be defined by:

$$Q_{\mathrm{t}} = Q_{\mathrm{fd}} + Q_{\mathrm{wd}} \tag{6}$$

where Q_{t} is the total interrill sediment transport, and Q_{fd} is the raindrop-induced and overland flow-driven sediment transport. Although this study involved evaluating both rainsplash transport and overland flow transport under wind-driven rains, only results of the rainsplash transport are presented in this paper, which aims to provide a better basis for modeling rainsplash transport.

2. Materials and methods

The study was conducted in a wind tunnel rainfall simulator facility at Ghent University, Belgium (Gabriels et al., 1997a). A continuous spraying system of downward-oriented nozzles was used, and nozzle pressure was kept at 1.50 bar. The nozzles at this operating pressure delivered a median drop size of 1.61, 1.54 and 1.54 mm for the rains driven by the reference wind velocities of 6.0, 10.0 and 12 m s^{-1}, respectively. Simulated rainfalls driven by horizontal wind velocities of 6.0, 10.0 and 12 m s^{-1} were applied to 20 × 55-cm soil pans under freely drained conditions for a 45-min duration. The slope gradients were 4.0°, 8.5° and 11.3° (7%, 15% and 20%, respectively) facing both windward and leeward directions (Fig. 1).

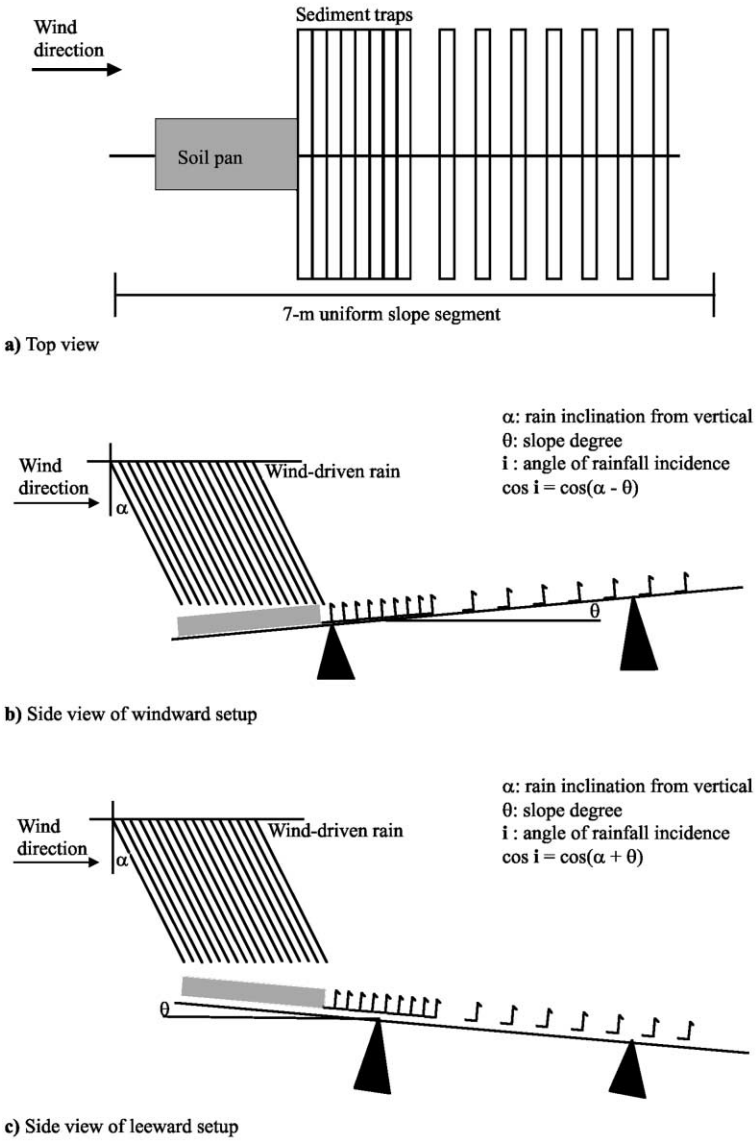

Fig. 1. Experimental set-up with the soil pan and sediment traps for rainsplash measurement arranged on the slopes of windward and leeward in the wind tunnel.

The impact velocity of the wind-driven raindrops was measured by the splash cup technique (Ellison, 1947). The reason for using this method rather than the distrometer (Analyser AM-90; Distrometer RD-69) was the fact that the distrometer was highly affected by the wind sound in the tunnel and did not work in the wind-driven rains. The impact velocities of the median drop sizes for the rains driven by the reference wind

velocities of 6.0, 10.0 and 12 m s^{-1} were 2.8, 5.4 and 6.0 m s^{-1}, respectively. A detailed description of the raindrop distribution and impact velocities for the rains of wind tunnel is given in Erpul et al. (1998, 2000).

Rain intensity was directly measured with five small collectors placed next to the soil pan and with the same slope gradient and aspect as the soil pan during the simulated rain. In this way, the intensity measurements were made truly representative of each run without any need for correction. A trigonometric model (Sharon, 1980; De Lima, 1990) was used to calculate the angle of rainfall incidence from the rain inclination, slope gradient and slope aspect:

$$\cos i = \cos(\alpha - \theta), \text{ for windward} \tag{7}$$

$$\cos i = \cos(\alpha + \theta), \text{ for leeward} \tag{8}$$

where θ is the slope gradient (°), and α is the rain inclination from the vertical (°). The angle of rain inclination was 52°, 66° and 67° for the wind-driven rain with 6.0, 10.0 and 12.0 m s^{-1}, respectively (Gabriels et al., 1997b). The angles refer to the mean values generalized over raindrop size range.

Raindrop impact pressure for the median drop size was calculated from the impact velocity and the angle of rainfall incidence. In the present study, we assumed that the rainsplash detachment rate under wind-driven rain is related to the normal component of raindrop impact velocity (Eq. (1)). The number of drops Ξ (#) is calculated from rain intensity, I (m s^{-1}) and exposure time, t (s):

$$\Xi = IAt/\forall \tag{9}$$

where A is the surface area of the soil pan (m^2), $\forall$ is the volume of a raindrop, $\pi d^3/6$, (m^3). Eq. (3) is then used to calculate the total rain impact pressure.

The reference wind velocities were measured up to 2 m with a vane-type anemometer and associated recording equipment. The wind velocity profiles for reference wind velocities are characterized by following logarithmic equation:

$$u_z = (u_*/\kappa)\ln(z/z_o) \tag{10}$$

where u_z is the wind velocity (m s^{-1}) at height z (m), u_* is the wind shear velocity (m s^{-1}), κ is von Karman's constant, and z_o is the roughness height (m). The boundary layer was set at about 0.20 m. Subsequently, the reference shear velocities are derived from the logarithmic wind profiles by regression, assuming a fixed roughness height of 0.0001 m for a bare and smoothed soil surface:

$$z = ae^{bu} \tag{11}$$

where $a = z_o$ and $b = \kappa/u_*$. Calculated reference shear velocities are 0.35, 0.53 and 0.77 m s^{-1} for the reference wind velocities of 6, 10 and 12 m s^{-1}, respectively.

The effect of rain load on the reference wind velocities was unknown during the wind-driven rain simulations because the velocity measurements were carried out without rain. We expect that the rain could alter the state of the wind, and the velocity could drop to a lower value than the corresponding wind velocity due to the extra drag exerted by the wind

on the raindrops. Unfortunately, anemometers suitable to work under rainy conditions were not available during the simulations. Therefore, the rainless wind velocity profiles were used to predict rainsplash transport rate under wind-driven rain.

Three agricultural soils, Kemmel1 silt loam (28.9% sand, 58.6% silt and 12.5% clay) and Kemmel2 loam (37.8% sand, 44.4% silt and 17.7% clay) from the Kemmelbeek watershed (Heuvelland, West Flanders, Belgium), and Nukerke silt loam (22.2% sand, 60.1% silt and 17.8% clay) from the Maarkebeek watershed (Flemish Ardennes, East Flanders, Belgium) were used in this study. The soil samples were collected from the A_p horizon and air-dried prior to the experiment. Soil was sieved into three aggregate fractions: 1.00–2.75, 2.75–4.80 and 4.80–8.00 mm, and the weighing factors assigned to each fraction were 28%, 32% and 40%, respectively. A 5-kg soil sample was then packed loosely into a 55-cm-long and 20-cm-wide pan after three fractions of aggregates were evenly mixed.

On each soil for one aspect with three replicates, 27 runs (total of 162 rainfall simulations) were performed. Transport rates were measured by trapping the splashed particles at set distances in the upslope and downslope directions, respectively, for windward and leeward slopes. The soil trapped in the collecting troughs (Fig. 1) was washed into beakers, oven-dried and weighed. Rainsplash transport rate was estimated from the area under the curves of mass with distance (Fig. 2) by:

$$Q_{\mathrm{wd}} = \frac{1}{At_a} \int m_i \mathrm{d}x \tag{12}$$

where Q_{wd} is the rainsplash transport rate (g m^{-1} s^{-1}); A is the collecting trough area (m^2) with trough length, $L = 1.20$ m and trough width, $W = 0.14$ m; m_i is the mass of soil (g)

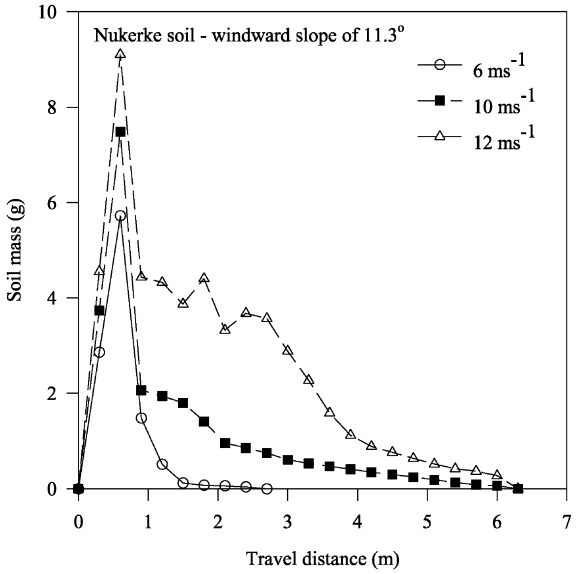

Fig. 2. Mass distribution curves used for calculating the rainsplash transport rate and the center of gravity. Mean rain intensities were 113, 142 and 120 mm h^{-1} for the rains driven by the reference wind velocities of 6, 10 and 12 m s^{-1}, respectively.

splashed over the distance x_i (m); t_a is the time (s) during which the rainsplash process occurred. The product of At_a determines the number of particles (# m^{-2} s^{-1}), which are raindrop-induced and entrained in the splash droplets.

Since soil particles left the surface with different initial lift-off speeds and angles, the prediction of particle trajectories was considered as an average in this study. We used the first moment of the mass distribution curves (Van Heerden, 1967), which is the center of gravity of the curves, to approximate the mean rainsplash distance:

$$\sum_{i=1}^{n} (x_i - X)m_i = 0 \tag{13}$$

and

$$X = \frac{\sum_{i=1}^{n} x_i m_i}{\sum_{i=1}^{n} m_i} \tag{14}$$

where X is the mean rainsplash distance (m), and the other variables are as defined previously.

3. Results and discussion

3.1. Rain impact pressure

Wind-driven rains impacted the sloping soil surface differentially, depending on wind velocity and direction. Results for the impact pressures of wind-driven rains are presented in Table 1 as a function of the raindrop impact velocity, impact angle and impact frequency. In essence, the angle of rain incidence, which varied as a function of rain inclination, and slope gradient and aspect, illustrated two effects on rain impact pressure. The first one was on the raindrop impact angle. For a given wind velocity, and hence rain inclination and impact velocity, the incidence decreased in windward while increasing in the leeward slopes as the slope gradient increased (Eqs. (7) and (8)). Since the impact angle is inversely related to the angle of incidence, which is measured from the normal to the sloping test surface, it decreased as the angle from the vertical increased. Therefore, the raindrop impact pressure, p_d, which was related to the normal component of the impact velocity, decreased while the angle of incidence increased (Table 1).

The second effect was on the raindrop impact frequency: the inclined rain gauge measurements indicated that the rain amount, which was actually intercepted, decreased as the angle of incidence increased (Sharon, 1980; De Lima, 1990). In our experimental set-up, the raindrop impact frequency depended not only upon the angle of incidence but also upon the number and the configuration of nozzles in the test area. Because of different raindrop trajectories, the test area received rain only from one nozzle in the rains driven by

Table 1
Summary of data for raindrop characteristics and those used in evaluating the impact pressures of wind-driven rains

u	u_*	v	α	θ	i	p_d (kPa)	I (mm h^{-1})	d_{50} (mm)	Ξ	Γ (MPa)
(m s^{-1})			(°)							
6 ww	0.35 ($0.27 \le u_* \le 0.44$)[a]	2.8 ($2.1 \le v \le 3.4$)	52	4.0	48	3.44	91 (8)	1.61	1229	4.23
				8.5	44	4.05	105 (6)	($1.38 \le d_{50} \le 1.84$)	1411	5.72
				11.3	41	4.43	113 (10)		1526	6.76
10 ww	0.53 ($0.47 \le u_* \le 0.60$)	5.4 ($5.0 \le v \le 5.8$)	66	4.0	63	6.27	126 (10)	1.54	2053	12.86
				8.5	58	8.26	138 (13)	($1.50 \le d_{50} \le 1.57$)	2246	18.55
				11.3	55	9.57	142 (16)		2311	22.11
12 ww	0.77 ($0.69 \le u_* \le 0.86$)	6.0 ($5.8 \le v \le 6.2$)	67	4.0	63	7.17	94 (10)	1.54	1479	10.60
				8.5	59	9.55	114 (8)	($1.51 \le d_{50} \le 1.57$)	1789	17.09
				11.3	56	11.12	120 (11)		1879	20.90
6 lw	0.35 ($0.27 \le u_* \le 0.44$)	2.8 ($2.1 \le v \le 3.4$)	52	4.0	56	2.40	124 (9)	1.61	1672	4.01
				8.5	61	1.85	107 (17)	($1.38 \le d_{50} \le 1.84$)	1436	2.66
				11.3	64	1.54	98 (8)		1316	2.02
10 lw	0.53 ($0.47 \le u_* \le 0.60$)	5.4 ($5.0 \le v \le 5.8$)	66	4.0	71	3.28	90 (6)	1.54	1471	4.82
				8.5	75	1.97	61 (4)	($1.50 \le d_{50} \le 1.57$)	998	1.96
				11.3	78	1.32	52 (5)		843	1.11
12 lw	0.77 ($0.69 \le u_* \le 0.86$)	6.0 ($5.8 \le v \le 6.2$)	67	4.0	71	3.64	65 (5)	1.54	1022	3.72
				8.5	76	2.12	43 (4)	($1.51 \le d_{50} \le 1.57$)	680	1.44
				11.3	79	1.38	41 (7)		649	0.89

u: Horizontal wind velocity (ww: windward and lw: leeward); u_*: wind shear velocity; v: drop impact velocity; α: rain inclination from the vertical; θ: slope gradient; and i: angle of rain incidence calculated by Eqs. (7) and (8) for windward and leeward slopes, respectively, using the rain inclination and the slope degree.
p_d: Raindrop impact pressure calculated by Eq. (1).
I: Rain intensity measured on the inclined plane relative to the prevailing wind direction. These measurements were simultaneously taken with the runs and represent a mean of 45 measurements of every rain inclination, slope degree and aspect combination. Standard deviation is given inside the parentheses.
d_{50}: Median drop size.
Ξ: Number of drops impacting on the source area per unit time calculated by Eq. (9).
Γ: Total rainfall impact pressure calculated by Eq. (3).
[a] 95% confidence interval on mean values of u_*, v and d_{50} are given inside the parentheses.

the wind velocity of 6 m s^{-1} and from two nozzles in the rains driven by wind velocities of both 10 and 12 m s^{-1}. This fact, to some degree, masked the effect of the angle of incidence on the raindrop impact frequency in windward slopes. For example, there was an unexpected increase in the intensity in the rains driven at 10 and 12 m s^{-1} when compared to the intensity of the rains driven by the wind velocity of 6 m s^{-1} although the angle of incidence was considerably greater. This sudden increase in the intensity was because of the two nozzles that provided rain with the soil surface in the rains driven at 10 and 12 m s^{-1}. However, when the test area received the rain from the same number of nozzles, the influence of the angle of incidence on the rain interception was obvious in the windward slopes. On the other hand, in leeward slopes, due to the expectation of dramatic decreases in the rain interception as the incidence increases, the placement of the test area was changed to be able to catch an appreciable rain amount on the sloping soil surface. Because of this, the intensity of rain driven by the wind velocity of 6 m s^{-1} was greater in the leeward slope of 4° than that in the windward slope. However, in this aspect, the fact that the angle of incidence attained the values approximately from 60° to 80° could not conceal the impairing effect of the angle of incidence on the rain interception even when the test area received rain from a different number of nozzles. It followed that the intensity gradually decreased as the incidence increased and reached very low values of approximately 40 mm h^{-1}. For example, the rain intensity measured in the windward slope of 11.3° was three times greater than that of the leeward slope for the runs driven by the wind velocity of 12 m s^{-1}. The important point here is that when the probability of the wind to accompany rain is high, the raindrop impact angle and frequency could widely vary with wind velocity and direction, leading to different rain impact pressures on different facing and sloping surfaces. The results for the calculated rain impact pressures are plotted in Fig. 3. The plots indicate that lower rain impact pressures corresponded with the leeward slopes. Differences in the rain impact pressure between the aspects were extremely large in

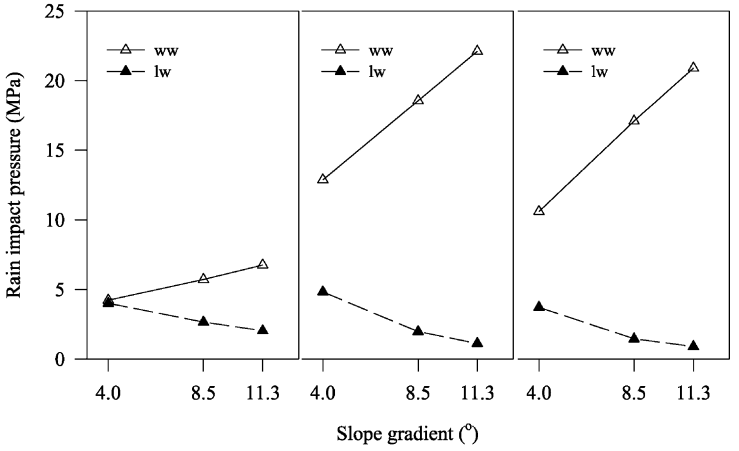

Fig. 3. Variations in rain impact pressure influenced by velocity, angle and frequency of the raindrop impact (ww: windward and lw: leeward).

the runs of 10 and 12 m s^{-1}. Fig. 3 also shows that slope gradient acts differentially on the rain impact pressure: it gradually increased and decreased, respectively, in wind- and leeward slopes as the slope gradient increases.

3.2. Rainsplash transport rate

Measured rainsplash rates varied in close relationship to the rain impact pressure and wind shear velocity. Values for three soils are presented in Table 2. Similar results were obtained for all three soils. The plot of rainsplash transport rate vs. the rain impact pressure at each level of the wind shear velocity are indicated in the three curves of different slopes (Fig. 4). Here, the data are fitted to the linear curves with different slopes. At the levels of wind shear velocities of both 0.53 and 0.77 m s^{-1}, the coefficients of determination, R^2, were equal to or greater than 0.90. However, those at 0.35 m s^{-1}, the R^2 were 0.76, 0.63 and 0.33 for Nukerke, Kemmel1 and Kemmel2, respectively. The reason for these relatively lesser values is the fact that we were confined to a very narrow pressure range at this level, and the data points were not really adequate to fit a regression line. In spite of this, it was apparent from the results that the transport rates were greatest when rain impact pressure and wind shear velocity were greatest. The following model was developed for the rainsplash transport rate by the log–linear regression analysis (SAS, 1995):

$$Q_{wd} = K\Gamma^a u_*^b \tag{15}$$

where Q_{wd} is expressed in units of g m^{-1} s^{-1}, Γ in units of MPa, and u_* in units of m s^{-1}. K, a and b are the model parameters. The statistical fit of this power law model is shown in Table 3 and Fig. 5 for the three soils and for all data regardless of soil type.

The analysis of variance showed that K, a and b were significant at the $P=0.0001$ level of significance for the three soils. Statistical analyses also revealed that at the level of $\alpha=0.05$, the exponents a and b for all soils are not significantly different from 1 and 2, respectively. Eq. (15) could thus be simplified to:

$$Q_{wd} = K\Gamma u_*^2 \tag{16}$$

Eq. (16) reflects the combined effect of rain and wind on the rainsplash transport process and suggests that the rate at which soil particles are set into motion in the air is a function of raindrop impact pressure. Subsequently, the wind velocity gradient will determine the travel distance.

3.3. Prediction of mean rainsplash distance

To understand the raindrop-induced and wind-driven soil particle transport, it is important to acquire knowledge on how distance traveled by a particle depends on the wind velocity profile. The amount of rainsplash trapped in the troughs at set distances along a 7-m uniform slope section indicated that particle trajectories were complete at 3 m in the rains driven by 6 m s^{-1} wind velocity and at 6 m in the rains driven by wind velocities of both 10 and 12 m s^{-1}. The calculated mean rainsplash distances, X, are given in Table 2. In all cases, X slightly changed with slope gradient and aspect and tended to

Table 2
Measured rainsplash transport rates (Q_{wd}) and mean rainsplash distances (X) approximated by the center of gravity for the three soils studied

Slope aspect	θ (°)	u (m s^{-1})	Nukerke		Kemmel1		Kemmel2		n
			Q_{wd} (g m^{-1} s^{-1})	X (m)	Q_{wd} (g m^{-1} s^{-1})	X (m)	Q_{wd} (g m^{-1} s^{-1})	X (m)	
Windward	4.0	6	3.76e − 02 (3.60e − 03)[a]	0.61 (0.02)	3.37e − 02 (1.84e − 03)	0.60 (0.03)	1.23e − 02 (8.44e − 04)	0.69 (0.12)	3
		10	1.05e − 01 (4.54e − 03)	1.25 (0.16)	1.20e − 01 (1.91e − 02)	1.29 (0.38)	8.91e − 02 (1.60e − 02)	1.35 (0.28)	3
		12	3.11e − 01 (2.46e − 02)	1.92 (0.18)	2.98e − 01 (1.81e − 02)	1.85 (0.06)	2.18e − 01 (4.66e − 02)	1.99 (0.29)	3
	8.53	6	3.65e − 02 (4.51e − 03)	0.73 (0.03)	3.24e − 02 (3.19e − 03)	0.66 (0.04)	3.27e − 02 (4.60e − 03)	0.65 (0.04)	3
		10	1.84e − 01 (7.39e − 03)	1.12 (0.37)	1.78e − 01 (2.35e − 02)	1.47 (0.63)	1.79e − 01 (2.52e − 02)	1.11 (0.14)	3
		12	6.43e − 01 (7.52e − 02)	1.66 (0.20)	4.41e − 01 (4.08e − 02)	1.89 (0.12)	7.18e − 01 (1.91e − 01)	1.84 (0.05)	3
	11.31	6	4.68e − 02 (5.33e − 03)	0.61 (0.05)	3.16e − 02 (1.97e − 03)	0.65 (0.05)	1.97e − 02 (7.67e − 04)	0.66 (0.04)	3
		10	1.67e − 01 (1.67e − 02)	1.37 (0.55)	1.74e − 01 (1.85e − 02)	1.42 (0.39)	1.43e − 01 (3.59e − 02)	1.26 (0.11)	3
		12	5.01e − 01 (9.51e − 02)	1.86 (0.46)	6.81e − 01 (5.02e − 02)	1.90 (0.09)	6.64e − 01 (1.30e − 01)	2.06 (0.12)	3
Leeward	4.0	6	3.75e − 02 (3.37e − 03)	0.74 (0.03)	2.12e − 02 (1.60e − 03)	0.73 (0.13)	2.52e − 02 (1.50e − 03)	0.68 (0.17)	3
		10	4.79e − 02 (3.34e − 03)	1.06 (0.16)	4.09e − 02 (2.50e − 03)	1.15 (0.16)	4.46e − 02 (2.15e − 03)	0.99 (0.14)	3
		12	1.43e − 01 (6.30e − 03)	1.51 (0.19)	1.39e − 01 (9.48e − 03)	1.83 (0.06)	1.01e − 01 (7.30e − 03)	1.59 (0.09)	3
	8.53	6	2.73e − 02 (1.07e − 03)	0.62 (0.04)	2.18e − 02 (1.25e − 03)	0.76 (0.03)	1.88e − 02 (5.96e − 04)	0.73 (0.06)	3
		10	2.50e − 02 (1.46e − 03)	1.40 (0.13)	1.93e − 02 (2.49e − 03)	1.14 (0.22)	2.43e − 02 (1.37e − 03)	1.10 (0.18)	3
		12	5.72e − 02 (5.34e − 03)	1.87 (0.19)	3.18e − 02 (3.75e − 03)	1.66 (0.12)	3.46e − 02 (4.74e − 03)	1.62 (0.05)	3
	11.31	6	9.74e − 03 (8.33e − 04)	0.70 (0.01)	1.86e − 02 (1.97e − 03)	0.77 (0.03)	8.14e − 03 (9.43e − 04)	0.71 (0.04)	3
		10	1.17e − 02 (1.93e − 03)	0.95 (0.06)	1.59e − 02 (1.70e − 03)	1.04 (0.07)	1.78e − 02 (7.49e − 04)	0.94 (0.07)	3
		12	2.33e − 02 (3.16e − 03)	1.82 (0.27)	2.28e − 02 (2.47e − 03)	1.80 (0.15)	1.93e − 02 (2.88e − 03)	1.69 (0.18)	3

[a] Standard deviation for Q_{wd} and X is given inside the parentheses.

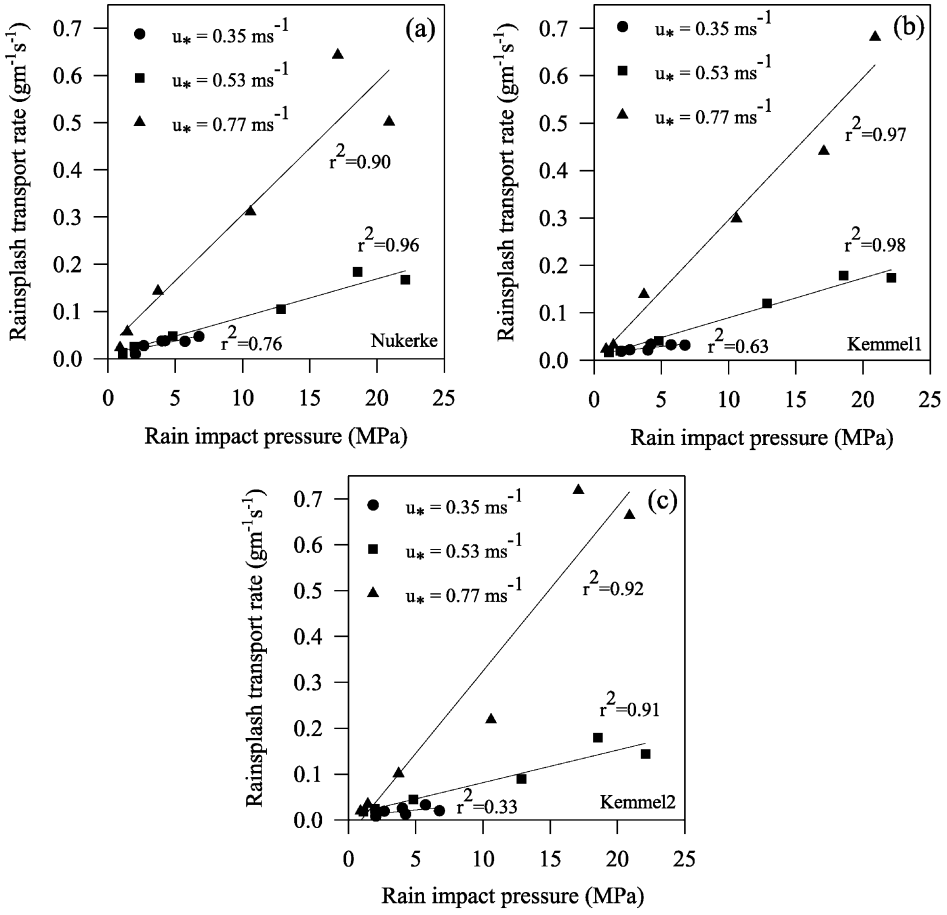

Fig. 4. Rainsplash transport rate as a function of rain impact pressure evaluated at the each wind shear velocity level for Nukerke silt loam (a), Kemmel1 silt loam (b) and Kemmel2 loam (c).

decrease in the leeward slopes. However, this tendency was not significant. Although the effect of slope gradient and aspect on the mean rainsplash distance appeared insignificant at a given shear velocity, a significant difference emerged as shear velocity increased.

Table 3
Statistical analyses of the rainsplash transport rate equation (*) developed by log–linear regression technique

Soil	K	Prob>|T|	a	Prob>|T|	b	Prob>|T|	R^2
Nukerke	0.05	0.0001	0.91	0.0001	1.84	0.0001	0.93
Kemmel1	0.05	0.0001	0.91	0.0001	1.85	0.0001	0.95
Kemmel2	0.05	0.0001	0.93	0.0001	2.28	0.0001	0.94
All data	0.05	0.0001	0.92	0.0001	1.99	0.0001	0.93

* $Q_{wd} = K\Gamma^a u_*^b$.

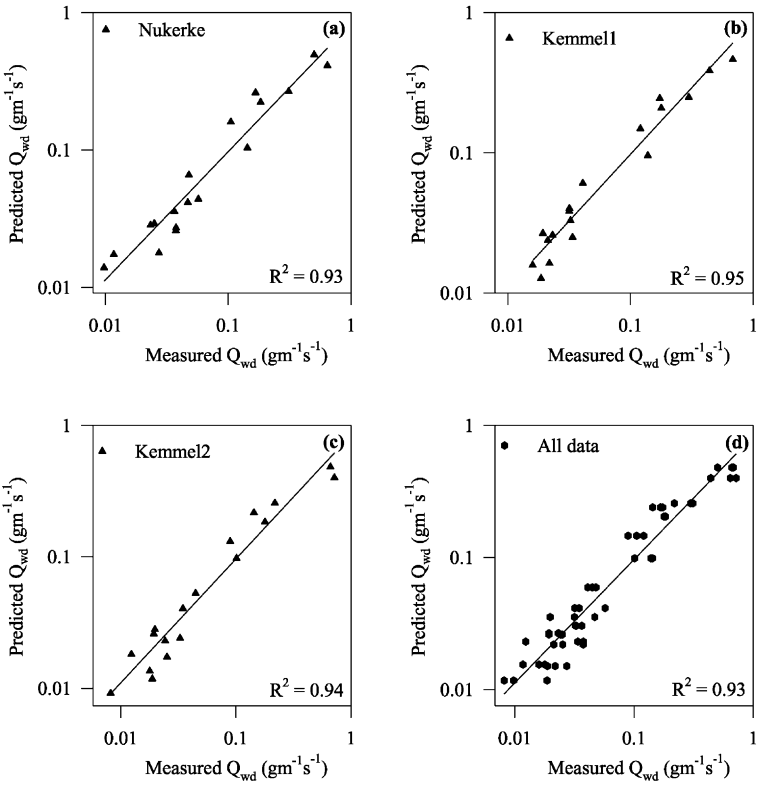

Fig. 5. Measured and predicted rainsplash transport rates of Nukerke silt loam (a), Kemmel1 silt loam (b), Kemmel2 loam (c) and all data regardless of soil type (d) using a log–linear regression.

These calculations suggest that wind had a significant effect on the deviation of the trajectories towards the direction of the wind (De Lima, 1989) and increased the fall distances of particles in the wind direction (Moeyersons, 1983; Moss and Green, 1983).

The rainsplash mechanism by which particles are entrained in the splash droplets and those ejected with initial velocity and the trajectories over which droplets travel are to some degree intricate and uncertain (Zaslavsky and Sinai, 1981; Reeve, 1982; Al-Durrah and Bradford, 1982). Bagnold (1941) estimated the initial vertical speed of particle lift-off to be in the order of the wind shear velocity. Owen (1980) thus described the saltation trajectory of a typical sand particle with a height of 0.81 (u_*^2/g) and a length of 10.3 (u_*^2/g), where g is the gravitational acceleration. This prediction is based on an assumed vertical lift-off speed of a sand particle. Our experimental data showed that $Q_{wd} \propto u_*^2$, and that is mainly affecting the direction and extent of rainsplash erosion, and also that wind did not contribute to the initiation of particle movement except as it changes velocity, angle and frequency of the raindrop impact. If we further assume that the splash droplet experiences the effect of gravity in the vertical direction (Maeno et al., 1979), the quantity of (u_*^2/g) then represents the momentum loss per unit time per unit length of travel per unit lateral

Table 4
Statistical analyses of the mean rainsplash distance equation (*) developed by non-linear regression technique

Soil	Parameter	95% Confidence interval		R^2
	C_1	Lower	Upper	
Nukerke	32.3	28.8	35.9	0.90
Kemmel1	33.4	29.7	37.1	0.92
Kemmel2	32.3	29.0	35.6	0.92
All data	32.7	30.8	34.6	0.91

* $X = C_1(u_*^2/g)$.

dimension (Bagnold, 1941; Greeley and Iversen, 1985). As a result, for the description of the average path of raindrop-induced splash droplet, a statistical analysis was conducted with non-linear regression model of:

$$X = C_1(u_*^2/g) \tag{17}$$

where X is expressed in unit of m, u_* in units of m s^{-1}, and g in units of m s^{-2}. C_1 is a model parameter. The statistical fit of this function is shown in Table 4 for the three soils, and the mean rainsplash distances calculated by the center of gravity were plotted vs. predicted values by $C_1(u_*^2/g)$ in Fig. 6. Eq. (17) shows the fit of the data collected in this

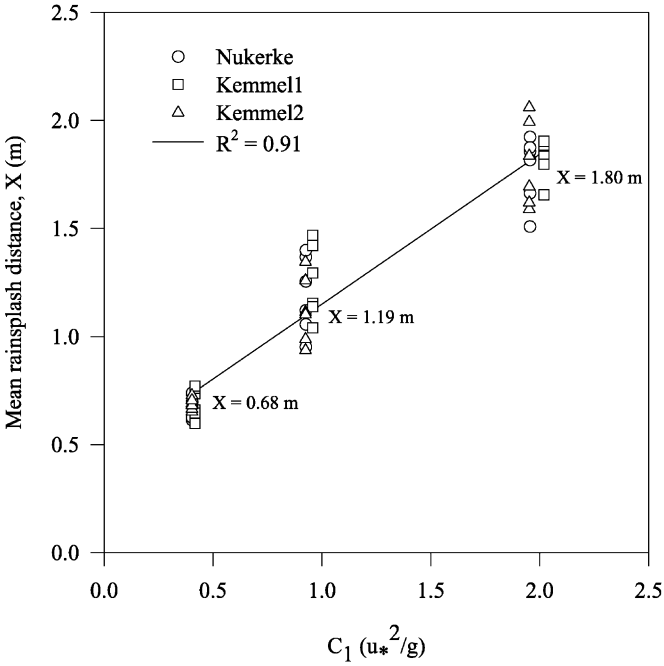

Fig. 6. Relationship between measured and predicted mean rainsplash travel distance using $C_1(u_*^2/g)$.

study, and for all data, C_1 is equal to 32.7 ± 1.9. An important point here is that the average trajectory of the raindrop-induced particle movement is approximately three times greater than the trajectory of a typical sand particle (White and Schulz, 1977; Owen, 1980). Longer particle trajectory might result from a change in the ejection velocity of the droplets (Ghadiri and Payne, 1980; Huang et al., 1982) and lower density of soil aggregates. The greater lift-off speeds are probably caused by the raindrop impact than that by hitting sand grains. Therefore, raindrop-induced particles could attain greater heights and travel longer distances.

4. Conclusions

A wind tunnel study under wind-driven rains was conducted to determine the combined effect of rain and wind on the rainsplash transport process. We termed this process as a raindrop-induced and wind-driven particle transport process. Transport by this process for the three soils studied was adequately described ($R^2 = 0.93$ for all data) using log–linear regression technique by Eq. (16), relating transport rate to the rain impact pressure and wind shear velocity. Eq. (16) reflects the combined effect of rain and wind on the process and also illustrates the twin effect of wind: one is on the detachment by changing the raindrop impact pressure, and the other is on transport by carrying the detached and lifted soil particles. Therefore, a model of this form could provide the basis for modeling interrill rainsplash transport under wind-driven rains, a common phenomenon in erosion events.

Average trajectory of a raindrop-induced and wind-driven particle was also adequately predicted by $32.7(u_*^2/g)$, and the travel distance is found three times greater in raindrop-induced process than the path of a typical saltating sand grain. We ascribed this to the greater lift-off speeds possibly caused by the raindrop impact and the lower densities of the soil aggregates.

The path of an individual splash droplet once it is injected into the air not only depends upon the wind velocity but can vary widely depending on the size and density of a particle. Therefore, more detailed research into the trajectory of the particles in the process is needed. On the other hand, the results of this laboratory work are valid for the conditions in which the experiments were conducted. Research is thus required for field testing of the laboratory results as well.

References

Al-Durrah, M.M., Bradford, J.M., 1981. New methods of studying soil detachment due to water drop impact. Soil Sci. Soc. Am. J. 45, 949–953.

Al-Durrah, M.M., Bradford, J.M., 1982. The mechanism of raindrop splash on soil surfaces. Soil Sci. Soc. Am. J. 46, 1086–1090.

Analyser AM-90. Distromet P.O. Box 33, CH-4020, Basel, Switzerland.

Bagnold, R.A., 1941. The Physics of Blown Sand and Desert Dunes. Methuen, London, 256 pp.

De Lima, J.L.M.P., 1989. Raindrop splash anisotropy: slope, wind, and overland flow velocity effects. Soil Technol. 2, 71–78.

De Lima, J.L.M.P., 1990. The effect of oblique rain on inclined surfaces: a nomograph for the rain-gauge correction factor. J. Hydrol. 115, 407–412.

De Lima, J.L.M.P., Van Dijck, P.M., Spaan, W.P., 1992. Splash–saltation transport under wind-driven rain. Soil Technol. 5, 151–166.

Disrud, L.A., Krauss, R.K., 1971. Examining the process of soil detachment from clods exposed to wind-driven simulated rainfall. Trans. ASAE, 90–92.

Distrometer RD-69. Distromet P.O. Box 33, CH-4020, Basel, Switzerland.

Ellison, W.D., 1947. Soil erosion studies (7 parts). Agric. Eng. 28, 145–146, 197–201, 245–248, 297–300, 349–351, 407–408, 447–450.

Erpul, G., Gabriels, D., Janssens, D., 1998. Assessing the drop size distribution of simulated rainfall in a wind tunnel. Soil Tillage Res. 45, 455–463.

Erpul, G., Gabriels, D., Janssens, D., 2000. The effect of wind on size and energy of small simulated raindrops: a wind tunnel study. Int. Agrophys. 14, 1–7.

Gabriels, D., Cornelis, W., Pollet, I., Van Coillie, T., Quessar, M., 1997a. The ICE wind tunnel for wind and water erosion studies. Soil Technol. 10, 1–8.

Gabriels, D., Tack, K., Erpul, G., Cornelis, W.M., Norton, L.D., Biesemans, J., 1997b. Effect of wind-driven rain on splash detachment and transport of a silt loam soil: a short slope wind tunnel experiment. In: Proc. Int. Workshop on Technical Aspects and Use of Wind Tunnels for Wind-Erosion Control. Combined Effect of Wind and Water on Erosion Processes. I.C.E. Special Report No. 1, Int. Centre Eromology, November 17–18, 1997, Ghent, Belgium, pp. 87–93.

Ghadiri, H., Payne, D., 1980. A study of soil splash using cine-photography. In: De Boodt, M., Gabriels, D. (Eds.), Assessment of Erosion. Wiley, Chichester, pp. 185–192.

Ghadiri, H., Payne, D., 1981. Raindrop impact stress. J. Soil Sci. 32, 41–49.

Greeley, R., Iversen, J.D., 1985. Wind as a Geological Process on Earth, Mars, Venus, and Titan. Cambridge Univ. Press, New York, NY 10022, USA.

Hairsine, P.B., Rose, C.W., 1991. Rainfall detachment and deposition: sediment transport in the absence of flow-driven processes. Soil Sci. Soc. Am. J. 55, 320–324.

Heymann, F.J., 1967. A survey of clues to the relation between erosion rate and impact parameters. In: Proc. Int. Conf. on Rain Erosion and Allied Phenomena. Second Rain Erosion Conference, The Royal Aircraft Establishment, Farnborough, England, 2, pp. 683–760.

Huang, C., Bradford, J.M., Cushman, J.H., 1982. A numerical study of raindrop impact phenomena: the rigid case. Soil Sci. Soc. Am. J. 46, 14–19.

Jungerius, P.D., Dekker, L.W., 1990. Water erosion in the dunes. Catena 18, 185–193, Suppl.

Jungerius, P.D., Verheggen, A.J.T., Wiggers, A.J., 1981. The development of blowouts in De Blink, a coastal dune area near Noordwijkerout, The Netherlands. Earth Surf. Processes Landforms 6, 375–396.

Kinnell, P.I.A., 1991. The effect of flow depth on sediment transport induced by raindrops impacting shallow flows. Trans. ASAE 34, 161–168.

Lyles, L., Disrud, L.A., Woodruff, N.P., 1969. Effects of soil physical properties, rainfall characteristics, and wind velocity on clod disintegration by simulated rainfall. Soil Sci. Soc. Am. Proc. 33, 302–306.

Lyles, L., Dickerson, J.D., Schmeidler, N.F., 1974. Soil detachment from clods by rainfall: effects of wind, mulch cover, and initial soil moisture. Trans. ASAE 17, 697–700.

Maeno, N., Araoka, K., Nishimuma, K., Kaneda, Y., 1979. Physical aspect of the wind–snow interaction in blowing snow. J. Fac. Sci. 6, 127–141.

Moeyersons, J., 1983. Measurements of splash–saltation fluxes under oblique rain. Catena 4, 19–31, Suppl.

Moeyersons, J., De Ploey, J., 1976. Quantitative data on splash erosion simulated on unvegetated slopes. Z. Geomorph. 25, 120–131.

Morgan, R.P.C., 1978. Field studies of rainsplash erosion. Earth Surf. Processes 3, 295–299.

Moss, A.J., Green, P., 1983. Movement of solids in air and water by raindrop impact: effects of drop-size and water-depth variations. Aust. J. Soil Res. 21 (3), 373–382.

Owen, P.R., 1980. Sand movement mechanism. Workshop on Physics of Desertification. International Center for Theoretical Physics, Trieste, Italy.

Parsons, A.J., Abrahams, A.D., Wainwright, J., 1994. Rainsplash and erosion rates in an interrill area on semi-arid grassland, Southern Arizona. Catena 22, 215–226.

Pedersen, H.S., Hasholt, B., 1995. Influence of wind speed on rainsplash erosion. Catena 24, 39–54.
Poesen, J., 1981. Rainwash experiments on the erodibility of loose sediments. Earth Surf. Processes Landforms 6, 285–307.
Poesen, J., 1985. An improved splash transport model. Z. Geomorphol. 29, 193–221.
Poesen, J., 1986. Field measurements of splash erosion to validate a splash transport model. Z. Geomorphol., Suppl. 58, 81–91.
Poesen, J., Savat, J., 1981. Detachment and transportation of loose sediments by raindrop splash: Part II. Detachability and transportability measurements. Catena 8, 19–41.
Reeve, I.J., 1982. A splash transport model and its application to geomorphic measurement. Z. Geomorphol. 26, 55–71.
SAS, 1995. SAS System for Elementary Statistical Analysis. SAS Institute, Cary, NC, USA, pp. 280–285.
Schultz, J.P., Jarrett, A.R., Hoover, J.R., 1985. Detachment and splash of a cohesive soil by rainfall. Trans. ASAE 28, 1878–1884.
Sharma, P.P., Gupta, S.C., Foster, G.R., 1995. Raindrop-induced soil detachment and sediment transport from interrill areas. Soil Sci. Soc. Am. J. 59, 727–734.
Sharon, D., 1980. The distribution of hydrologically effective rainfall incident on sloping ground. J. Hydrol. 46, 165–188.
Springer, G.S., 1976. Erosion by Liquid Impact. Wiley, New York.
Torri, D., Sfalanga, M., Del Sette, M., 1987. Splash detachment: runoff depth and soil cohesion. Catena 14, 149–155.
Umback, C.R., Lembke, W.D., 1966. Effects of wind on falling water drops. Trans. ASAE 9, 805–808.
Van Heerden, W.M., 1964. Splash erosion as affected by the angle of incidence of raindrop impact. Unpublished PhD thesis. Purdue University, Lafayette, IN, USA.
Van Heerden, W.M., 1967. An analysis of soil transportation by raindrop splash. Trans. ASAE 10, 166–169.
White, B.R., Schulz, J.C., 1977. Magnus effect on saltation. J. Fluid Mech. 81, 497–512.
Wright, A.C., 1987. A physically based model of the dispersion of splash droplets ejected from a water drop impact. Earth Surf. Processes Landforms 11 (4), 351–367.
Zaslavsky, D., Sinai, G., 1981. Surface hydrology: distribution of raindrops. J. Hydraul. Div., Am. Soc. Civ. Eng. 107, 17–36.